An article submitted to Journal of Geophysical Research Oceans

Contribution of biological effects to carbonate-system variations and the air–water CO_2 flux in inner and outer bays in Japan

Tatsuki Tokoro*[,1,2], Shin-ichiro Nakaoka[1], Shintaro Takao[1], Tomohiro Kuwae[2], Atsushi Kubo[3], Toru Endo[4], Yukihiro Nojiri[1,5]

[1]Center for Global Environmental Research, National Institute for Environmental Studies, Tsukuba, Japan

[2]Coastal and Estuarine Environment Research Group, Port and Airport Research Institute, Yokosuka, Japan

[3]Department of Geosciences, Shizuoka University, Shizuoka, Japan

[4]Graduate School of Engineering, Osaka City University, Osaka, Japan

[5]Graduate School of Science and Technology, Hirosaki University, Hirosaki, Japan

Key points:

- Inner bays in Japan are reportedly annual atmospheric CO_2 sinks but comprehensive measurements are few.
- We quantified biological effects on carbonate parameters and CO_2 flux using an empirical relationship with riverine and oceanic endmembers.
- The biological effect was regulated mainly by nutrient concentrations related to wastewater treatment.

*Corresponding author: Tatsuki Tokoro (tokoro.tatsuki@nies.go.jp)

Abstract

We evaluated the contribution of biological effects (photosynthesis, respiration, and decomposition) to the carbonate parameters and air–water CO_2 fluxes in Tokyo Bay, Ise Bay and Osaka Bay in Japan. The carbonate parameters were measured mainly by cargo ships travelling between Japan and other countries. We used the measurement data from three inner bays and surrounding outer bays in Japan along with reference data from previous studies for complementary analysis. We found that 1) the inner bays in this study were strong annual atmospheric CO_2 sinks, 2) the annual biological effect on the air–water CO_2 fluxes was about 5–25% of the measured CO_2 fluxes and it affected the seasonal variation of the CO_2 flux, and 3) the biological effect was largest in Tokyo Bay, and almost the same in Ise and Osaka Bays. The intensity of the biological effect corresponded mainly with nutrient concentrations, which seemed to be controlled by the wastewater treatment in urbanized areas around the bays. The CO_2 flux was also affected by the seawater residence time, salinity, and stratification. Our results suggest that labile carbon/nutrient ratio of wastewater should be a major consideration for evaluating the biological effect on the carbon cycle in urbanized inner bays, which will continue to expand globally.

Plain Language Summary

We analyzed the biological effect (photosynthesis, respiration, and decomposition) on air–water CO_2 exchange in Tokyo Bay, Ise Bay and Osaka Bay in Japan using data from cargo-ship measurements and previously published reports. We concluded that 1) bay water strongly absorbs atmospheric CO_2, 2) biological effects accounted for 5–25% of the evaluated CO_2 absorption and had significant effects on its seasonal variation, and 3) the biological effects seemed to be mediated mainly by the carbon/nutrient ratio in wastewater. This study should improve our understanding of the carbon flow in urbanized coastal areas, which are expanding globally.

1. Introduction

The ocean is one of the largest carbon reservoirs on earth, and the quantification of the exchange of atmospheric carbon dioxide (CO_2) with the ocean is necessary for predicting future climate change. The air–water CO_2 flux in the major oceans has been studied since the late 1970s and the regional and seasonal variations have been estimated (e.g., Takahashi et al., 2009; Wanninkhof et al., 2019). Meanwhile, the quantification of the flux in coastal areas is still challenging because of the large temporal and spatial variations. Recent studies have shown that near-shore areas are sources of atmospheric CO_2 on average because of the input and of organic carbon and the mineralization (Borges et al., 2005; Cai, 2011; Chen and Borges, 2009; Chen et al., 2013), whereas some other studies showed a local annual CO_2 sink in areas with submerged autotrophic ecosystems (Kayanne et al., 1995; Tokoro et al., 2014). Marginal seas (continental shelves) have been reported as atmospheric CO_2 sinks but there is still uncertainty surrounding the actual estimates has been debated (Borges et al., 2005; Cai, 2011; Chen and Borges, 2009; Chen et al., 2013; Laruelle et al., 2014).

The role of inner and outer bays in atmospheric CO_2 exchange has not been analyzed comprehensively despite their importance in anthropogenic activities (Chen and Borges, 2009; Chen et al., 2013). Although the near-shore area is generally considered to be a CO_2 source region, some studies have reported that urbanized inner bays in Japan are annual atmospheric CO_2 sinks (Endo et al., 2017; Fujii et al., 2013; Kubo et al., 2017). In these bays, CO_2 undersaturation might result from wastewater treatment (Kubo et al., 2017; Kuwae et al., 2016). The treatment process removes labile carbon, yielding water with relatively less carbon than nutrients, which promotes primary production in the bay water. In addition, the organic matter remaining in the treated water is refractory (Kubo et al., 2015) and thus further mineralization and increase in the CO_2 concertation in the bay water is suppressed. However, the effects of biological processes such as photosynthesis, respiration, and decomposition on the carbonate parameters and the air–water CO_2 flux have not been precisely quantified.

Here, we evaluated the biological effects of inner-bay water on temporal and spatial changes in the carbonate parameters and the air–water CO_2 flux, including the surrounding outer bays, in Japan. We discuss the biological effects on the flux in terms of the regulating factors and the extendibility or our observations to other areas and for global estimation.

2. Methodology

2.1 Study site

This study took place in Japan in Tokyo Bay, Ise Bay, and Osaka Bay, and surrounding areas (Figure 1). These bays have similar topographic conditions such as a southward entrance to the bay open to the Pacific Ocean and a surrounding, highly urbanized coastal area. The populations of the urban areas surrounding Tokyo, Ise and Osaka Bays were 37, 9 and 19 million, respectively, in 2014 (Global Metro Monitor; https://www.brookings.edu/research/global-metro-monitor/). In this study, the term “bay” refers to the inner and outer areas of each bay, which were analyzed together for expedience.

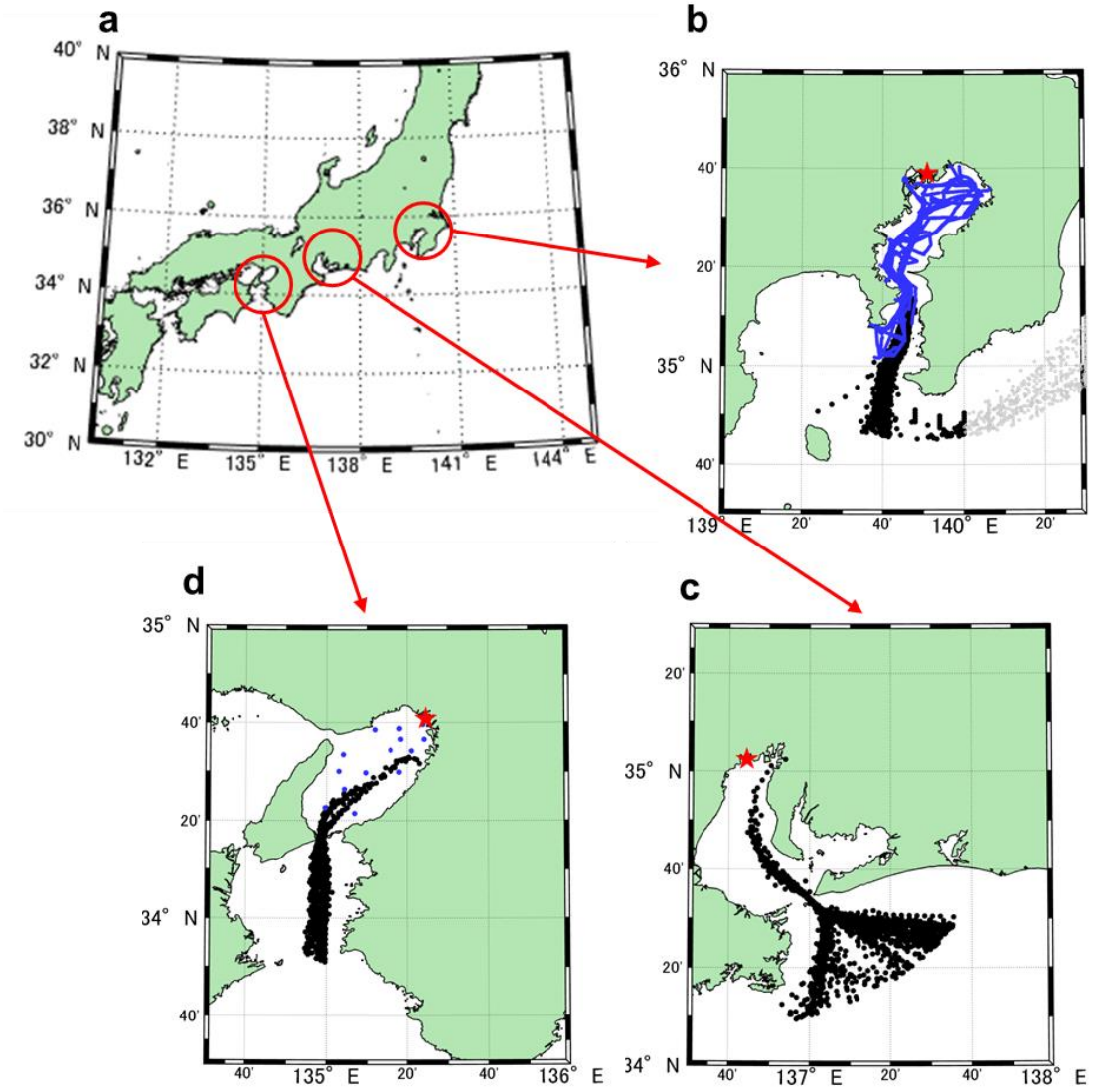

Figure 1. (a) Map of Japan and the general locations of the bays and surrounding seas included in this study. (b) Tokyo Bay, (c) Ise Bay, (d) Osaka Bay. The black filled circles indicate the locations of the National Institute for Environmental Studies (NIES) data used in this study. The grey circles in (b) are filtered NIES data from east of 140°E, which were defined as data external to Tokyo Bay. The blue circles indicate additional data collected by Tokyo University of Marine Science and Technology (TUMSAT) in Tokyo Bay and by Osaka City University (OCU) in Osaka Bay. The red stars mark the river mouths of the main river located in the inner part of each bay and used as the zero point for the distance parameter *dist* (Tokyo Bay, 35.65°N, 139.85°E; Ise Bay, 35.04°N, 136.74°E; Osaka Bay, 34.68°N, 135.41°E).

2.2 Data processing

The data used for this study are measurements of water temperature, salinity and fugacity of CO_2 (fCO_2) in the main urbanized inner bays and in the surrounding outer bays, as observed by the National Institute for Environmental Studies (NIES), Tokyo University of Marine Science and Technology (TUMSAT) and Osaka City University (OCU). The other carbonate parameters—total alkalinity (TA) and dissolved inorganic carbon (DIC)—were estimated using an empirical relationship between TA and salinity, and the equilibrium calculation. The biological effect on carbonate parameters and the air–water CO_2 flux was calculated from the difference between the above estimated DIC and the value from the conservative mixing line between the oceanic and riverine endmembers. We quantified the air–water CO_2 flux and the magnitude of the biological effect to evaluate the contribution of the biological effect in the bays to the exchange of atmospheric CO_2.

The water temperature, salinity, and fCO_2 in water and air were obtained from the NIES database (https://soop.jp). The data are also available from the Surface Ocean CO_2 Atlas (SOCAT; http://www.socat.info), which has been a public database since 2011 and represents an international collaboration among research institutes. The NIES observations implemented as the Voluntary Observing Ship (VOS) programs by cargo ships were originally for understanding the global carbon cycle but their data also include inner bay measurements from 2005 to 2016 in Tokyo Bay and Ise Bay and from 2011 to 2016 in Osaka Bay, where the cargo ships taking measurements have anchor stations. We first extracted the data for 30–40°N and 130–145°E observed by the cargo ships as the original coastal data. The details on fCO_2 measurements are reported by Nakaoka et al. (2013).

For complementary analysis, we included some previous data as more

landward information than the NIES data. For Tokyo Bay, we added the data collected by TUMSAT from 2007 to 2010 (Kubo et al., 2017) to the NIES data after converting pCO_2 to fCO_2 using the empirical relationship incorporating temperature (Körtzinger, 1999). Likewise, for complementary analysis, we added more landward measurement data from Osaka Bay collected by OCU in spring and autumn of 2014 (Endo et al., 2017). The additional raw data for Osaka Bay included the water temperature, salinity, and DIC. We therefore estimated fCO_2 using the equilibrium calculation (Zeebe and Wolf-Gladrow, 2001; we used their "recommended" coefficients for the calculation) and the TA from the empirical relationship with salinity (Taguchi et al., 2009).

The data were filtered by the distance from the inner part of each bay. The distance parameter *dist* (km) was calculated as follows:

$$dist = 6370 \times \sqrt{(lat - dist0\_lat)^2 + (lon - dist0\_lon)^2 \times \cos\left[\left(\frac{lat+dist0\_lat}{2}\right)^2\right]} \quad (1)$$

where *lat* and *lon* are the latitude and longitude of the measurement point in radians, respectively. *dist0_lat* and *dist0_lon* are the latitude and longitude of the point representing the mouth of the river with the highest flow among the rivers in the inner part of each bay (Ara River in Tokyo Bay, Kiso River in Ise Bay, and Yodo River in Osaka Bay; Figure 1). The data for which *dist* > 100 km were excluded from analysis as being out-of-range of the inner and outer bays, as determined by changepoint analysis using the salinity and DIC (see Text S1). In addition, the data from Tokyo Bay with longitude >140°E were excluded because even though these data were within the range of *dist* ≤ 100 km, they were from locations on the opposite side of a peninsula from the inner bay (Figure 1). In total, we analyzed 18,118 data points from Tokyo Bay (16,924 from TUMSAT), 1926 from Ise Bay and 1067 from Osaka Bay (28 from OCU).

Because the NIES data for the inner bays were distributed uni-dimensionally along the course of the cargo ships, the spatial information for the data in this study was standardized by the distance parameter *dist* mentioned above. For evaluating seasonality, we calculated the parameter *monthlydata* for each data point using the temporal information as follows:

$$monthlydata = month + \frac{(day-1)}{365.25} \times 12 \quad (2)$$

where *month* and *day* are the month (1–12) and day (1–28 or 30 or 31) of the

measurement, respectively. Additionally, given the temporal and spatial heterogeneity of the measurement data, we used natural neighbor interpolation (Sibson, 1981) to interpolate a grid with values at intervals of 1 km (*dist*) and 0.1 (*monthlydata*). In order for the interpolation to reflect the seasonal cycle from the minimum and maximum values for *monthlydata* (on 1 January and 31 December, respectively), the interpolation was performed with the data from the latter half of the year (July to December) added before the start of original data and that from the first half (January to June) appended to the end.

In order to minimize the effect of the trend in fCO_2 due to anthropogenic CO_2 input to the ocean, we corrected for the increase rate in each bay and in the additional data, except for the OCU data because those measurements were only taken for a single year. The linear increase rate for each bay was estimated from the annual average fCO_2. The increase in fCO_2 in water was corrected to that in 2010 if the increase was significant. The linear rates of fCO_2 increase in water were 5.83 and 3.24 μatm yr^{-1} in Tokyo and Ise Bay, respectively, and were significant ($p < 0.001$), whereas that in Osaka Bay was not significant ($p = 0.64$). Also, the additional TUMSAT data for Tokyo Bay showed no significant increase ($p = 0.85$). Therefore, the rate of increase was corrected to the base year of 2010 only for NIES data for Tokyo Bay and Ise Bay. For fCO_2 in air, we assumed an increase of 1.5 μatm yr^{-1} and corrected to this from the base year value.

2.3 Calculation of the biological effect

Because fCO_2 in water is affected by temperature and salinity, the biological effect cannot be quantified using only carbonate-system parameters. Although some previous studies normalized fCO_2 using an empirical relationship between temperature and fCO_2 (e.g., Takahashi et al., 2009), such a technique cannot be applied to coastal carbonate analysis because the salinity varies widely and affects TA and DIC non-linearly. Instead, we evaluated the biological effect using DIC, which is a conservative parameter, and direct information about the biological effect from processes such as photosynthesis, respiration, and decomposition (Figure 2). The DIC was calculated using the carbonate equilibrium calculation (Zeebe and Wolf-Gladrow, 2001) with TA estimated from the empirical relationship with salinity in each bay from a previous study (Taguchi et al., 2009).

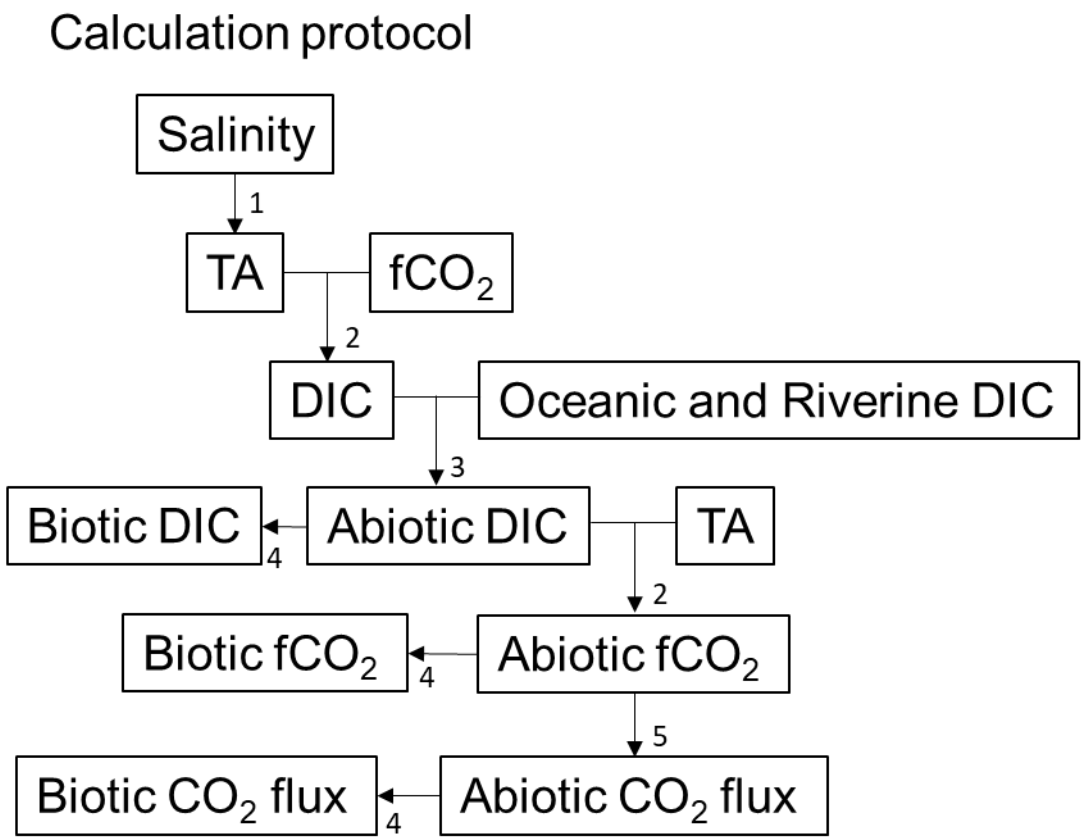

Figure 2. Procedure for calculating abiotic and biotic CO_2 flux. 1: Calculation of total alkalinity (TA) using the empirical relationship of Taguchi et al. (2009). 2: Carbonate equilibrium calculation (Zeebe & Wolf-Gladrow, 2001). 3: Calculation of abiotic dissolved inorganic carbon (DIC) using the interpolation of the oceanic and riverine endmembers. 4: Calculation of biotic parameters as the difference between the net parameter and the abiotic parameter. 5: Calculation using equation (4). fCO_2, CO_2 fugacity.

For quantifying the biological effect, we defined DIC_b as the increase or decrease in DIC through biological activities. The DIC_b was calculated as the difference between DIC estimated from the equilibrium calculation and DIC_{ab}, which was the interpolated value between the oceanic and riverine endmembers in the coordinate system of salinity and DIC (Tokoro et al., 2014). DIC_{ab} represents the DIC concentration resulting from the mixing of the endmembers without any additional change in the bays such as through biological activity.

The endmembers and the biological effect were determined as follows. 1) the salinity and DIC of the oceanic endmember were estimated as the value outside of the

respective outer bays. In this study, those values were estimated as the monthly average of the salinity and DIC between *dist* of 90 km and 100 km. 2) We assumed that biological activity reached a minimum ($DIC_b \approx 0$) in the winter period (here, the three months with the lowest average water temperatures), according to the positive correlation between production by seagrass and algae and water temperature (Davison, 1991; Lee et al., 2007; Tait & Schiel, 2013). Then the least-squares line of the salinity and DIC through the oceanic endmember average value during the above winter period can be used to approximate the DIC_{ab} in the winter period, and the riverine endmember (DICr, μmol kg^{-1}). That is, the former parameter is the approximation using the regression line of DIC vs salinity, and the latter parameter is the regression line value when the salinity is zero. These parameters can be estimated as follows:

$$DICr = \frac{\sum[(DIC_w - DIC_{ow})(Sal_w - Sal_{ow})]}{\sum[(sal_w - sal_{ow})^2]} \times (Sal_r - Sal_{ow}) + DIC_{ow} \quad (3)$$

Here Sal_w and DIC_w are the salinity and DIC in each bay during the three months with the lowest average water temperature. Sal_{ow} and DIC_{ow} are the mean values of the salinity and DIC, respectively, of the oceanic endmember during these three months. Sal_r is the salinity of the riverine endmember and assumed to be zero in this study. 3) DIC_{ab} in each month was calculated again as the linearly interpolated value between the endmembers. To evaluate the uncertainty of the estimated riverine DIC, we defined the range of DIC as ±200 μmol kg^{-1} (see Text S2) and calculated the precision of the range for the following procedures. 4) DIC_b was calculated as the difference between the estimated DIC and DIC_{ab}. 5) fCO_2 was calculated from the equilibrium calculation using DIC_{ab} as the fCO_2 without any biological effects (fCO_{2ab}) and fCO_{2b} (the difference between fCO_2 and fCO_{2ab}) as the fCO_2 change due to the biological effects in each bay.

The air–water CO_2 flux (*F*, μmol m^{-2} s^{-1} or mol m^{-2} yr^{-1}) was calculated as follows:

$$F = k \cdot S(fCO_{2water} - fCO_{2air}) \quad (4)$$

where *k* is the gas transfer velocity (m s^{-1}) and calculated as described in the next paragraph. *S* is the solubility of CO_2 in water (mol m^{-3} atm^{-1}) and estimated using an empirical equation using water temperature and salinity (Weiss, 1974). fCO_{2water} and fCO_{2air} are the fugacity of CO_2 in water and air (μatm), respectively. A positive value for

the flux indicates a CO_2 efflux to the atmosphere, and vice versa. The air–water CO_2 flux due to abiotic factors (F_{ab}) and the contribution of biological effect to the flux (F_b) were also calculated using fCO_{2water} calculated from fCO_{2ab} and $fCO_{2b,}$ instead of the fCO_{2water}, respectively. Because the temporal and spatial information for fCO_{2air} from TUMSAT did not completely correspond to that of fCO_{2water} measurements, the data were approximated by the data with the same *dist–monthlydata* grid information, which was calculated by natural neighbor interpolation using the original TUMSAT fCO_{2air} data. Because the OCU data did not include fCO_{2air} measurements, we used the average value of the NIES data for Osaka Bay (392.6 μatm) for the calculation.

The gas transfer velocity k (here, the units are cm hr^{-1}) was calculated as follows (Wanninkhof, 2014):

$$k = 0.251 \times {U_{10}}^2 \times \left({Sc}/{660}\right)^{-0.5} \quad (5)$$

where U_{10} (m s^{-1}) is the wind speed at the height of 10 m from the water surface. Sc is the Schmidt number, defined as the ratio of the CO_2 molecular diffusion coefficient to the dynamic viscosity of seawater; Sc of seawater can be calculated from an empirical equation using the water temperature (Jähne et al., 1987). The wind data were taken from the database of the NEDO Offshore Wind System (NeoWins; http://app10.infoc.nedo.go.jp/Nedo_Webgis/top.html), which is the open database of the wind simulator provided by the New Energy and Industrial Technology Development Organization (NEDO) for evaluating the efficiency of offshore wind power generation in Japan. The wind data were supplied as the wind rose data, monthly averaged data, and averaged wind profile data, with 500-m resolution. We took the monthly averaged data at 10-km intervals beginning at *dist* = 0 along the water course (Table S1). Because the monthly averaged data were supplied as the data for 60–140 m above the water surface, while the wind profile was at 10–200-m height, we calculated the monthly averaged data at 10-m height according to the power-law of wind profile as follows:

$$U_{10} = U_{60} \times \left({10}/{60}\right)^{n}$$

$$n = \frac{\log(U_{p60}/U_{p10})}{\log(60/10)} \quad (6)$$

where U_{60} (m s^{-1}) is the monthly averaged data at 60-m height. U_{p10} and U_{p60} are the

304 wind-profile data at 10-m and 60-m height, respectively (Pagon, 1935). The wind data
305 were applied to the carbonate measurement data for each of the 12 months and 10 km of
306 *dist*.
307
308 2.4 Data interpolation and error range
309
310 Because the measurement data were not homogeneous temporally or spatially,
311 the averages and deviations described in this study were calculated from the interpolated
312 data, which is a homogeneous grid of the distance (every 1 km *dist*) and date (every
313 0.1-*monthlydata*) data ($n = 100 \times 120 = 12{,}000$). The error values for the carbonate
314 parameters are shown in Table S2.
315 The procedure used for error estimation is described in the Supporting
316 Information (Text S3). The error propagation was complicated because of the
317 non-linearity of the carbonate equilibrium calculation, so the error was separated into
318 the random error mainly due to the TA estimation and the riverine error due to
319 uncertainty in estimating the riverine DIC.
320
321 **3. Results**
322
323 3.1 Temperature, salinity, and carbonate parameters
324
325 The water temperature and salinity (mean ± SD) in each bay were 19.15 ±
326 4.59 °C and 31.42 ± 3.39 (Tokyo Bay), 18.78 ± 5.36 °C and 31.97± 2.23 (Ise Bay), and
327 18.66 ± 5.12 °C and 31.88 ± 1.43 (Osaka Bay), respectively (Figure S1). fCO_2 was
328 305.56 ± 87.80 μatm (Tokyo Bay), 294.88 ± 46.38 μatm (Ise Bay), and 300.56 ± 70.30
329 μatm (Osaka Bay) (Figure 3). The estimated TA and DIC were 2161 ± 125 and 1872 ±
330 129 μmol kg^{-1} (Tokyo Bay), 2166 ± 115 and 1883 ± 120 μmol kg^{-1} (Ise Bay), and 2179
331 ± 64 and 1893 ± 85 μmol kg^{-1} (Osaka Bay) (Figure S2).
332

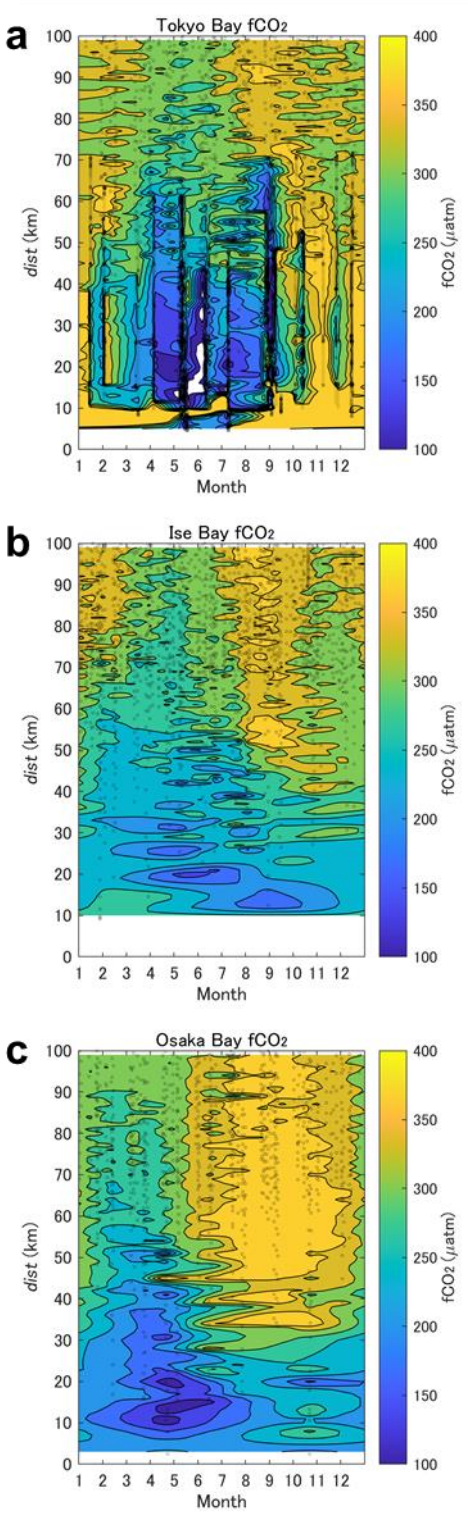

Figure 3. Temporal and spatial distributions of the fugacity of CO_2 (fCO_2) in (a) Tokyo, (b) Ise, and (c) Osaka Bays. The color indicates the interpolated 0.1-month × 1-km grid value. The gray dots show the distribution of direct measurements. The white area in (a) indicates extreme values that were excluded from the analysis for clarity. The parameter *dist* represents the distance from a zero

point in the mouth of the main river feeding the inner bay (equation [1] in the main text).

The salinity and DIC of the oceanic endmembers were calculated for each month as the average values between 90 and 100 km from the river mouth reference point in each bay: 34.34 ± 0.31 and 1968 ± 35 μmol kg^{-1} in Tokyo Bay, 34.19 ± 0.39 and 1978 ± 45 μmol kg^{-1} in Ise Bay, and 33.43 ± 0.66 and 1958 ± 45 μmol kg^{-1} in Osaka Bay, respectively. These values were higher during winter and lower during summer and were consistent with the results from an empirical equation derived for the Kuroshio stream area (Ishii et al., 2011) (Figure S3). The DIC of the riverine endmember was estimated to be 1162 ± 200 μmol kg^{-1} in Tokyo Bay, 675 ± 200 μmol kg^{-1} in Ise Bay, and 852 ± 200 μmol kg^{-1} in Osaka Bay.

The DIC_{ab} and DIC_b were 1899 ± 87 and –27 ± 64 μmol kg^{-1} in Tokyo Bay, 1896 ± 97 and –13 ± 28 μmol kg^{-1} in Ise Bay, and 1906 ± 55 and –13 ± 39 μmol kg^{-1} in Osaka Bay, respectively (Figure 4). The estimated DIC_b showed a significant decrease within 70 km from land in summer in all bays. Meanwhile, there was an increase in Tokyo Bay within about 10 km of land from October to January. The seasonal trend of photosynthetic activity (decrease in DIC_b) was almost the same among the bays. The magnitude and spatial distribution of the photosynthetic activity was the greatest in Tokyo Bay, where respiration and/or organic-matter decomposition (increase in DIC_b) were evident mainly in autumn to winter. In the other two bays, the magnitude and spatial distribution of DIC_b were almost the same, and smaller than in Tokyo Bay.

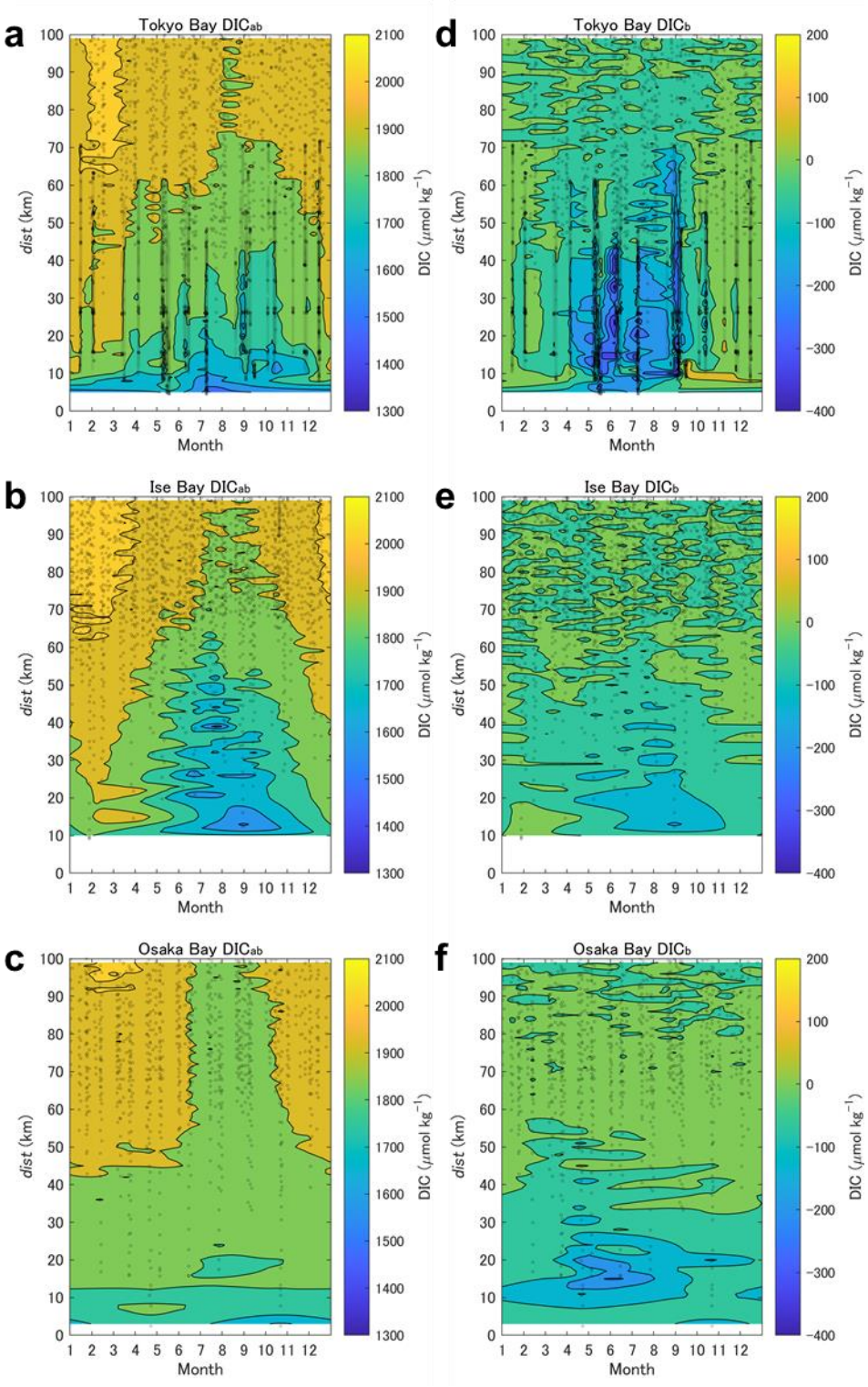

Figure 4. Temporal and spatial distributions of abiotic dissolved inorganic carbon (DIC_{ab}) ((a): Tokyo Bay, (b): Ise Bay, (c): Osaka Bay) and biotic DIC (DIC_b) ((d): Tokyo Bay, (e): Ise Bay, (f): Osaka Bay). The colors and dots are as defined in Figure 3. The parameter *dist* represents the distance from a zero point in the mouth of the main river feeding the inner bay (equation [1] in the

main text).

3.2 Air–water CO_2 fluxes

The air–water CO_2 fluxes in the three bays indicated that these areas were annual atmospheric CO_2 sinks (–2.87 ± 2.39, –3.20 ± 1.52 and –2.44 ± 1.71 mol m^{-2} yr^{-1} in Tokyo, Ise and Osaka Bays, respectively) (Figure 5). The temporal and spatial distribution of the air–water CO_2 flux in Ise and Osaka Bays were similar and showed a seasonal pattern whereas the distribution in Tokyo Bay seemed to be more consistent with that of DIC_b than a seasonal pattern (Figure 4). The peak of CO_2 absorption was during February to April, and CO_2 absorption was lowest in August and September in Ise and Osaka Bays, and in October and November in Tokyo Bay.

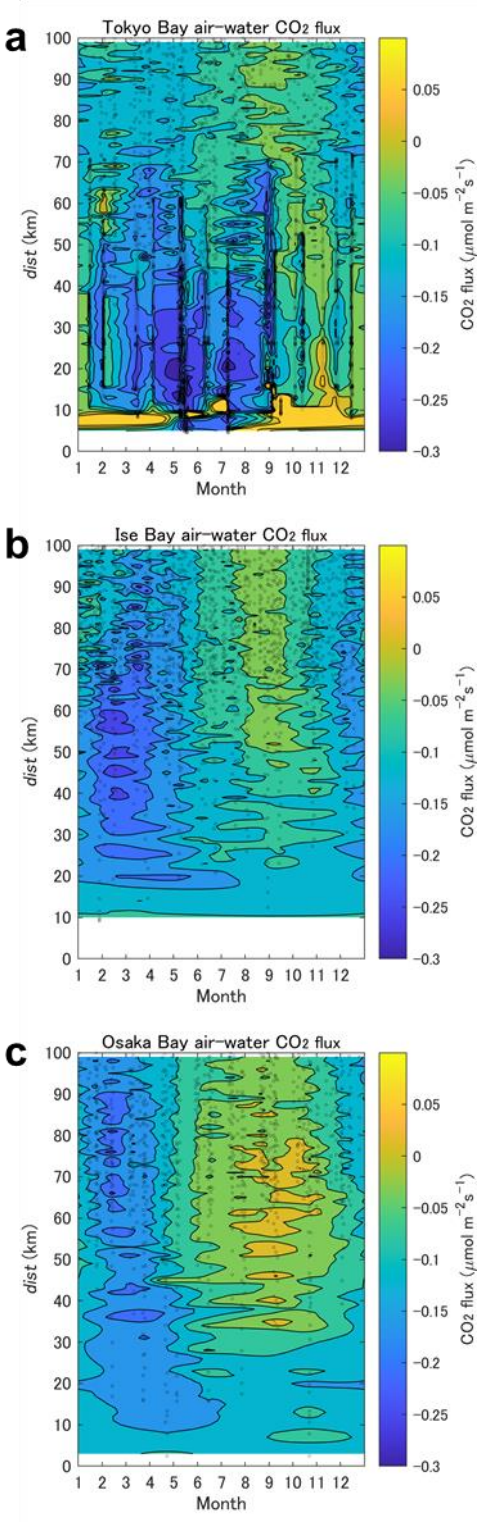

Figure 5. Temporal and spatial distribution of air–water CO_2 flux in (a) Tokyo, (b) Ise, and (c) Osaka Bays. The colors and dots are as defined in Figure 3. The parameter *dist* represents the distance from a zero point in the mouth of the main river feeding the inner bay (equation [1] in the main text).

The fluxes without (F_{ab}) and from biological activity (F_b) were –2.14 ± 1.75 and –0.73 ± 2.68 mol m^{-2} yr^{-1} (Tokyo Bay), –2.82 ± 1.73 and –0.38 ± 1.09 mol m^{-2} yr^{-1} (Ise Bay), and –2.31 ± 1.51 and –0.13 ± 1.09 mol m^{-2} yr^{-1} (Osaka Bay), respectively (Figure S4). The standard deviations of the biotic fluxes (F_b) indicated that the biological effect in Ise and Osaka Bays was weaker than in Tokyo Bay. The temporal and spatial distribution of F_{ab} showed a seasonal pattern whereas the distribution of F_b seemed to be related to the distribution of DIC_b.

4. Discussion

The validity of our estimates of biological effects on DIC (DIC_b) and CO_2 flux (F_b) depended on the precision of the riverine DIC endmember because the abiotic DIC (DIC_{ab}) and CO_2 flux (F_{ab}) were determined from the riverine endmember, along with the oceanic endmember whose error was relatively small. Although we could not find reasonable reference data for riverine DIC in the bays, the reported riverine TA data by Taguchi et al. (2009) which are 1006, 518 and 759 μmol kg^{-1} in Tokyo, Ise, and Osaka Bays, respectively, support the validity of the DIC estimation because water with a higher TA can contain more carbonate and bicarbonate ions as DIC under the same fCO_2 conditions. The range of estimated riverine fCO_2 in each bay also supports the validity of our estimates of riverine DIC and its precision (±200 μmol kg^{-1}) (see Text S2).

Our results support the hypothesized mechanisms related to wastewater treatment (Kubo et al., 2017; Kuwae et al., 2016). Typical wastewater treatment method removes carbon in the form of sludge and CO_2 gas more efficiently than nutrients such as nitrogen and phosphorus (Sedlak, 1991). Through these effluents, the balance of primary production and respiration in inner bay is offset towards an excess of primary production and the resultant suppression of fCO_2 increase. Second, the effluent contains relatively refractory carbon, because labile organic matter has already been removed by treatment (Kubo et al. 2015). Therefore, respiration and mineralization rates of effluent are low, and subsequent fCO_2 increases are suppressed.

The negative average annual biotic DIC in all three of the bays indicates that the ecosystems were net autotrophic. The magnitude of the biotic DIC seemed to be consistent with the nutrient concentrations reported in the reference material of the Ministry of the Environment, Japan

(https://www.env.go.jp/council/09water/y0917-07/ref02.pdf). In this report, the highest concentrations of total nitrogen and phosphorous were in Tokyo Bay, and were almost the same in Osaka and Ise Bays (average total nitrate, 0.8, 0.3, 0.4 mg L^{-1}; average total phosphate, 0.06, 0.03, 0.04 mg L^{-1} in Tokyo, Ise, and Osaka Bays, respectively). The nutrient concentrations in the three bays were probably determined by the volume of treated wastewater discharged into the bays, which is related to the size of the population of the surrounding urbanized area. For example, the inflow of the treated water is reported as the main component of the total freshwater inflow to Tokyo Bay and thus the effect of treated water should be noticeable on the nutrient concentration in the bays (Kubo et al., 2015). Although the net primary production in the bays depends on several parameters such as the seawater residence time and vertical stratification, its general magnitude would be similar to that of the biotic DIC because it is similarly influenced by hydrographic conditions.

It is possible that the net primary production in Osaka Bay was underestimated because Osaka Bay connects with the Seto Inland Sea at its landward end and this topography results in strong tidal currents in the bay (Odamaki, 2002). Stronger tides would enhance the water exchange between the bay and the surrounding areas and weaken the biological effects on DIC and the air–water CO_2 flux. In addition, the area at *dist* of 50–100 km coincides with narrow straits (Kitan Strait and Kii channel) where several large rivers flow into the bay. Thus, the calculation of the endmember effect in Osaka Bay might be biased compared with those for the other two bays.

The CO_2 fluxes found in this study indicate that the inner bays and surrounding outer bays in Japan are one of the largest atmospheric CO_2 sinks among the global coastal areas reviewed in previous studies (Borges et al., 2005; Chen and Borges, 2008). The overall average CO_2 flux for the bays (–2.84 mol m^{-2} yr^{-1}) is more negative than the average in these previous studies for estuaries (7.74–10.26 mol m^{-2} yr^{-1}) and marginal seas (continental shelves) (–1.64 to –1.06 mol m^{-2} yr^{-1}). The absorption in the bays was mainly based on the abiotic flux (75%, 88%, and 95% of the net CO_2 flux (*F*) in Tokyo, Ise, and Osaka Bays, respectively). The oceanic endmember from the Kuroshio stream area is the most plausible explanation for the CO_2 absorption (overall average CO_2 absorption of –2.32 mol m^{-2} yr^{-1}). That area has been reported as the one of the largest CO_2 sinks in the world because of the cooling effect of cold Oyashio water on warm Kuroshio water (Takahashi et al., 2002, 2009). We suggest that the CO_2 absorption in the bays was enhanced by additional cooling due to the terrestrial effect during winter (Figure S1).

The biotic CO_2 flux was the largest in Tokyo Bay, followed in order by Ise Bay

and Osaka Bay. The magnitude was basically the same as that of the biotic DIC and nutrient concentrations in each bay. The higher CO_2 absorption in Ise Bay compared to Osaka Bay despite almost identical biotic DIC can be explained by the lower salinity and TA in the near-shore area in Ise Bay (Figures S1 and S2). Because lower-TA water has less buffering effect on fCO_2, the decrease in fCO_2 in Ise Bay was greater than that in Osaka Bay even when the decrease in DIC was the same. Although the annual average of the biological effect was limited (25%, 12%, and 5% of the net CO_2 flux in Tokyo, Ise, and Osaka Bays, respectively), it affected the temporal and spatial distribution of the air–water CO_2 flux. Temporally, the pattern of F_b was the opposite of F_{ab}, with an influx (F_b) or efflux (F_{ab}) in summer and vice versa in winter (Figure 6). The biological effect was the strongest in Tokyo Bay and less notable in the other bays, as with the biotic DIC. As a result, the seasonal variation of the CO_2 flux in Tokyo Bay was different from that in the other two bays despite having almost the same variation in the abiotic CO_2 flux (Figure 6). For example, the peak CO_2 influx in winter in the bays continued into summer in Tokyo Bay, but the winter influx in Tokyo Bay was about two-thirds that in the other bays.

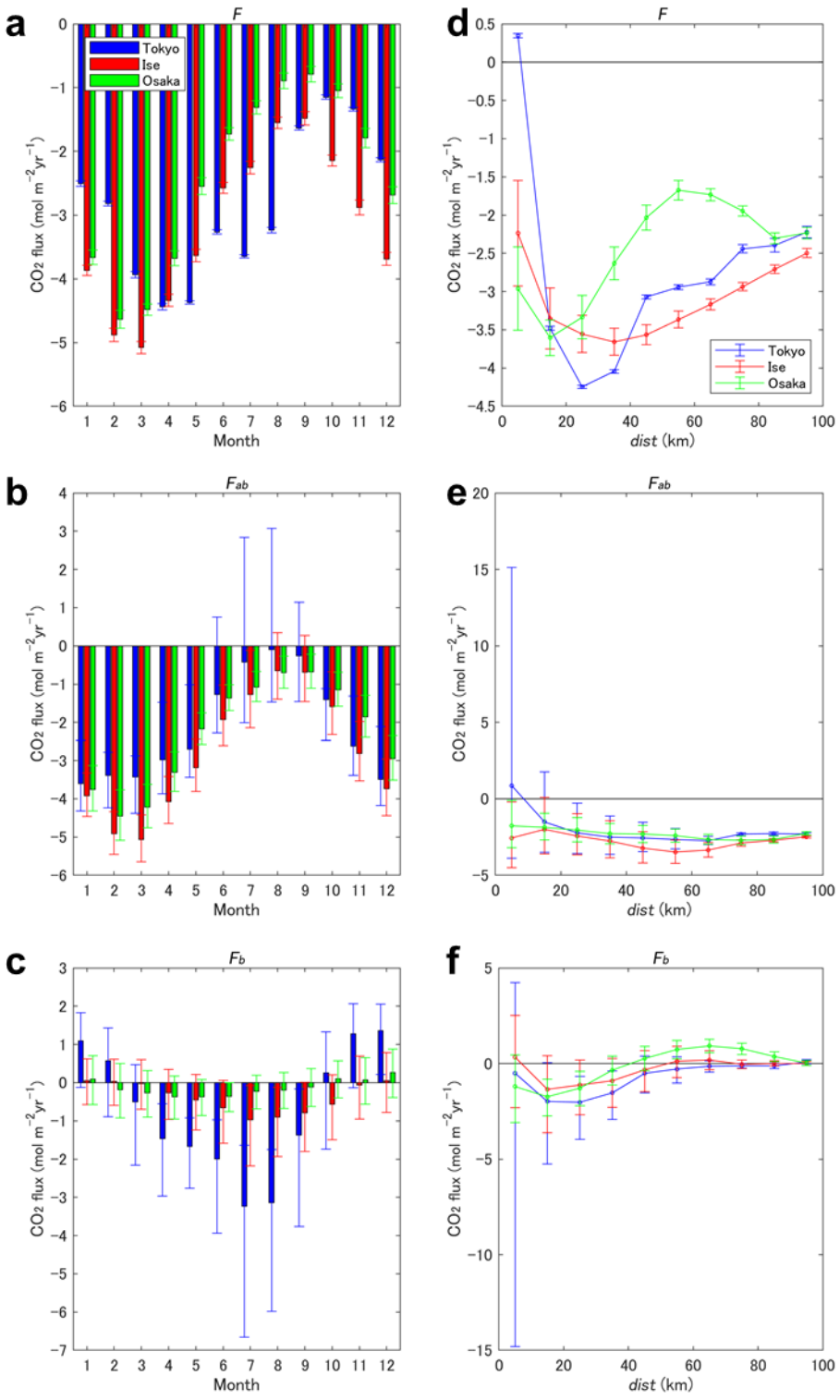

Figure 6. Temporal (left) and spatial (right) variations in the air–water CO_2 flux (F) ((a), (d)), abiotic flux (F_{ab}) ((b), (e)) and biotic flux (F_b) ((c), (f)). Note that the unit is different from Figure 5. The error bars were estimated by using equation (S4). The parameter *dist* represents the distance from a zero point in the mouth of the main river feeding the inner bay (equation [1] in the main text).

The difference in the spatial distribution of F_b among the bays was less noticeable than that in the temporal distribution because of the offset of the influx in summer and efflux in winter in Tokyo Bay (Figure 6). The magnitude of the influx peak at *dist* of about 20 km was almost the same among the bays whereas the efflux at *dist* > 50 km was the largest in Osaka Bay. This might be caused by the decomposition of the organic matter produced by the photosynthesis at about 20 km *dist*.

Meanwhile, there was limited CO_2 released to atmosphere in the near-shore area (*dist* ≤ 10 km) although fCO_2 of the riverine endmember was estimated at more than 2000–5000 μatm in the case of the intermediate riverine DIC (Figure 5). As for Tokyo Bay, there was a tendency toward an efflux in the near-shore area both in F_{ab} and F_b (Figure 6), corresponding to the decrease in the DIC_{ab} in summer and the increase in DIC_b in winter (Figures 4 and 5). Because the distribution of the decrease in DIC_{ab} was consistent with the salinity distribution (Figures 4 and S1), an increase in riverine flow from precipitation might cause a CO_2 release as an abiotic factor. On the other hand, the increase in DIC_b was consistent with the increase in pCO_2 observed in a previous study (Kubo et al., 2017) in which the increase was due to the weakening of stratification in Tokyo Bay due to the cooling of surface water, a decrease in precipitation, and the weakening of the seasonal southward wind. These factors probably contributed to bringing high-fCO_2 water and resuspended organic sediments from the bottom to the surface, resulting in the CO_2 efflux to the atmosphere. Although we could not perform a similar analysis for the other two bays because of a lack of measurement data, we would expect a similar, considerable efflux tendency because the other bays share the same hydrographic and climate conditions.

The comparison between Tokyo Bay and other two bays suggests that the enhanced urbanization results in increased biotic CO_2 absorption. Because the development of coastal areas will likely continue for several decades, the biotic absorption of CO_2 in the bays is expected to be a mitigating factor for future climate change. We assumed that the area within 100 km of the global coastline (6.2×10^7 km^2) could absorb atmospheric CO_2 additionally at the same rate as the biotic flux in Tokyo Bay (0.73 mol m^{-2} yr^{-1}), and roughly estimated the potential for additional biotic absorption to be 0.054 Pg yr^{-1}. This is on the same order of magnitude as the estimated estuarine CO_2 efflux (e.g., Chen et al., 2013). The estimation of worldwide abiotic CO_2 flux is difficult because the oceanic and riverine carbonate parameters differ at each location. In addition, the carbon export from urbanized areas is observed to increase along with the development (Barnes and Raymond, 2009; Lopes et al., 2020; Wang et

al., 2017). This increase in carbon export could mitigate the increase in biotic CO_2 absorption.

For accurate estimates of the global CO_2 absorption resulting from coastal urbanization, it is necessary to obtain more carbonate measurements from a variety of areas. For example, data from measurements at the lagoons in Ivory Coast and Guanabara Bay in Brazil suggested that strong CO_2 absorption and release are mixing in the tropical urbanized bay where the rate of wastewater treatment is low (Cotovicz et al., 2015; Koné et al., 2009). Both of these studies indicated that eutrophication and stratification were the factors regulating the undersaturation of CO_2. Meanwhile, studies in the Chesapeake Bay reported that both the absorption and release of CO_2 were observed by numerical simulation model and abundant pH measurement, respectively (Herrmann et al., 2020; St-Laurent et al., 2020). Because the main bottleneck for further study is the difficulty of obtaining comprehensive measurements in coastal areas, the development of novel methods like the above Chesapeake Bay studies will facilitate filling gaps in the temporal and spatial distributions of available data. The review study of such measurements is expected to understand the quantitative relationship between the coastal urbanization and the carbon cycle.

5. Conclusions

In this study we clarified the temporal and spatial variations of carbonate parameters in three bays in Japan from riverine water to the outer bays within a range of 100 km. Our results are the first to fill the gap between studies of nearshore areas and the marginal seas. We found a notable atmospheric CO_2 influx due to biological activity in the areas about 20 km from land in summer, accounting for 25%, 12%, and 5% of the measured net CO_2 flux in Tokyo, Ise, and Osaka Bays, respectively. In addition, the biological effect in the highly developed Tokyo Bay significantly affected the seasonal variation of air–water CO_2 flux. The potential for atmospheric CO_2 absorption was mainly regulated by the water in the surrounding marginal seas. The biological effect seemed to be associated with the nutrient concentrations, which are related to the volumes of treated wastewater entering the bays. In addition, the degree to which the water area is enclosed likely influences the biological effect. Conditions that are more closed or open would enhance or mitigate the biological effect on the air–water CO_2 flux, respectively.

This study should contribute to future investigations into the carbon cycle in

urbanized coastal areas, which will likely continue to expand for the next several decades. However, more detailed investigations in inner and outer bays are required for more precise evaluation of their contribution to the global carbon cycle. To expand the results of this study to the global scale will require further measurements in bays in a variety of regions.

Acknowledgements

We deeply appreciate the generous cooperation of Toyofuji Shipping Co. and Kagoshima Senpaku Co. with the NIES VOS program. We thank the captains and crews of M/S *Pyxis*, M/S *New Century 2*, M/S *Trans Future 5*, and TR/V *Shinyoumaru*. We appreciate the help of K. Watanabe and H. Moki at the Port and Airport Research Institute in their valuable comments for this study. This research was financially supported by Global Environmental Research Coordination System, Ministry of the Environment, Japan (grant number E1751).

References

Aufdenkampe, A. K., Mayorga, E., Raymond, P. A., Melack, J. M., Doney, S. C., Simone, R. A. et al. (2011). Riverine coupling of biogeochemical cycles between land, oceans, and atmosphere. *Frontiers in Ecology and the Environment*, 9(1), 53–60. https://doi:10.1890/100014

Barnes, R., & Raymond, P. A. (2009). The contribution of agricultural and urban activities to inorganic carbon fluxes within temperate watersheds. *Chemical Geology*, 266 (3), 318–327. https://doi:10.1016/j.chemgeo.2009.06.018

Borges, A. V., Delille, D., & Frankignoulle, M. (2005). Budgeting sinks and sources of CO_2 in the coastal ocean: Diversity of ecosystems counts. *Geophysical Research Letters*, 32, L14601. https://doi:10.1029/2005GL023053.

Cai, W.-J. (2011). Estuarine and coastal ocean carbon paradox: CO_2 sinks or sites of terrestrial carbon incineration? *Annual Review of Marine Science*, 3, 123–145. https://doi:10.1146/annurev-marine-120709–142723

Chen, C.-T. A., & Borges, A. V. (2009). Reconciling opposing views on carbon cycling in the coastal ocean: Continental shelves as sinks and near-shore ecosystems as source of atmospheric CO_2. *Deep Sea Research., Part II*, 56, 578–590. https://doi:10.1016/j.dsr2.2009.01.001

Chen, C.-T. A., Huang, T.-H., Chen, Y.-C., Bai, Y., He, X., & Kang, Y. (2013). Air-sea exchanges of CO_2 in the world's coastal seas. *Biogeosciences*, 10, 6509–6544. https://doi:10.5194/bg-10-6509-2013

Cotovicz Jr, L. C., Knoppers, B. A., Brandini, N., Costa Santos, S. J., & Abril, G. (2015). A strong CO_2 sink enhanced by eutrophication in a tropical coastal embayment (Guanabara Bay, Rio de Janeiro, Brazil). *Biogeosciences*, 12, 6125–6146, https://doi.org/10.5194/bg-12-6125-2015

Davison, J. R. (1991). Environmental effects on algal photosynthesis: *Temperature. Journal of Phycology*, 27, 2–8.

598 Endo, T., Shimano, J., Sakai, D., & Fujiwara, R. (2017). Relationship between vertical
599 distribution of pCO_2 in sea and air-sea CO_2 exchange in inner part of Osaka Bay.
600 *Journal of Japan Society of Civil Engineering., B2 coastal engineering*, 73 (2), I_1231–
601 1236.
602
603 Fujii, T., Fujiwara, T., & Nakayama, K. (2013). Fluxes of carbon dioxide in the eastern
604 regions of Osaka Bay. *Journal of Japan Society of Civil Engineering., B2 coastal*
605 *engineering*, 69 (2), I_1111–1115.
606
607 Herrmann, M., Najjar, R. G., Da, F., Friedman, J. R., Friedrichs M. A. M., Goldberger, S.
608 et al. (2020). Challenges in quantifying air-water carbon dioxide flux using estuarine
609 water quality data: case study for Chesapeake Bay. *Journal of Geophysical Research*
610 *Oceans*, 125 (7), e2019JC015610. https://doi.org/10.1029/2019JC015610
611
612 Ishii, M., Kosugi, N., Sasano, D., Saito, S., Midorikawa, T., & Inoue, H. Y. (2011).
613 Ocean acidification off the south coast of Japan: A result from time series observation of
614 CO_2 parameters from 1994 to 2008. *Journal of Geophysical Research*, 116, C06022.
615 https://doi:10.1029/2010JC006831
616
617 Jähne, B., Heinz, G., & Dietrich, W. (1987). Measurement of the diffusion coefficients
618 of sparingly soluble gases in water with a modified Barrer method. *Journal of*
619 *Geophysical Research*, 92, 10767–10776. https://doi:10. 1029/ JC092iC10p10767
620
621 Kayanne, H., Suzuki, A., & Saito, H. (1995). Diurnal changes in the spatial pressure of
622 carbon dioxide in coral reef water. *Science*, 269, 214–216. https://doi:
623 10.1126/science.269.5221.214
624
625 Koné, Y. J. M., Abril, G., Kouadio, K. N., Delille, B., & Borges, A. V. (2009). Seasonal
626 variability of carbon dioxide in the rivers and lagoons of Ivory Coast (West Africa).
627 *Estuaries and Coasts*, 32, 246–260. https://doi 10.1007/S12237-008-9121-0
628
629 Körtzinger, A. (1999). Determination of carbon dioxide partial pressure (pCO_2). In K.
630 Grasshoff, K. Kremling, M. Ehrhardt (Eds.), *Methods of Seawater Analysis* (pp. 149–
631 158), Weinheim: Wiley-VCH.
632
633 Kubo, A., Kawai, M. Y., & Kanda, J. (2015). Seasonal variations in concentration and

634 decomposition of dissolved organic carbon in Tokyo Bay, *Biogeosciences*, 12, 269–279.
635 https://doi.org/10.5194/bg-12-269-2015
636
637 Kubo, A., Maeda, Y., & Kanda, J. (2017). A significant net sink for CO_2 in Tokyo Bay.
638 *Scientific Reports*, 7:44355. https://doi: 10.1038/srep44355
639
640 Kuwae, T., Kanda, J., Kubo, A., Nakajima, F., Ogawa, H., Sohma, A., & Suzumura, M.
641 (2016). Blue carbon in human-dominated estuarine and shallow coastal systems. *Ambio*,
642 https://doi:10.1007/s13280-015-0725-x
643
644 Laruelle, G. G., Lauerwald, R., Pfeil, B., Regnier, P. (2014). Regionalized global budget
645 of the CO_2 exchange at the air-water interface in continental shelf seas. *Global*
646 *Biogeochemical Cycles*, 28, 1199–1214. https://doi: 10.1002/2014GB004832
647
648 Lee, K-S, Park, S. R., & Kim, Y. K. (2007). Effects of irradiance, temperature, and
649 nutrients on growth dynamics of seagrasses: A review. *Journal of Experimental Marine*
650 *Biology and Ecology*, 350 (1–2), 144–175. https://doi.org/10.1016/j.jembe.2007.06.016
651
652 Lopes, M. N., Decarli, C. J., Pinheiro-Silva, L., Lima, T. C., Leite, N. K. & Petrucio, M.
653 M. (2020). Urbanization increases carbon concentration and pCO_2 in subtropical
654 streams. *Environmental Science and Pollution Research*, 27, 18371–18381.
655 https://doi.org/10.1007/s11356-020-08175-8
656
657 Nakaoka, S., Telszewski, M., Nojiri, Y., Yasunaka, S., Miyazaki, C., Mukai, H., & Usui,
658 N. (2013). Estimating temporal and spatial variation of ocean surface pCO_2 in the North
659 Pacific using a self-organizing map neural network technique. *Biogeosciences*, 10,
660 6093–6106. https://doi.org/10.5194/bg-10-6093-2013
661
662 Odamaki, M. (2002). Improved co-tidal charts around Osaka Bay, Seto Inland Sea.
663 -Influence of Coriolis force on the tidal distribution-. *Report of Hydrographic*
664 *Researches*, 38, 85–99.
665
666 Pagon, W. W. (1935). Wind velocity in relation to height above ground. *Engineer's*
667 *News Record*, 114 (21), 742-751
668
669 Sedlak, R. I. (1991). *Phosphorus and nitrogen removal from municipal wastewater:*

principals and practice. Boca Raton: CRC Press.

Sibson, R. (1981). A brief description of natural neighbor interpolation. In V. Barnett (Eds.), *Interpreting Multivariate Data* (Chapter 2 pp.21–36), Chichester: John Wiley.

St-Laurent, P., Friedrichs, M. A. M., Najjar, R. G., Shadwick, E. H., Tian, H., & Yao, Y. (2020). Relative impacts of global changes and regional watershed changes on the inorganic carbon balance of the Chesapeake Bay. *Biogeosciences*, 17, 3779–3796. https://doi.org/10.5194/bg-17-3779-2020

Taguchi, F., Fujiwara, T., Yamada, Y., Fujita, K., & Sugiyama, M. (2009). Alkalinity in coastal seas around Japan. *Bulletin on Coastal Oceanography*, 47 (1), 71–75.

Tait, L. W., & Schiel, D. R. (2013). Impacts of temperature on primary production and respiration in naturally structured macroalgal assemblages, *PLos One*, 8 (9), e74413. https://doi: 10.1371/journal.pone.0074413

Takahashi, T., Sutherland, S. C., Sweeney, C., Poisson, A., Metzl, N., Tilbrook, B., et al. (2002). Global sea-air CO_2 flux based on climatological surface ocean pCO_2, and seasonal biological and temperature effects. *Deep Sea Research., Part II*, 49, 1601–1622. https://doi: 10.1016/S0967-0645(02)00003-6

Takahashi, T., Sutherland, S. C., Wanninkhof, R., Sweeney, C., Feely, R. A., Chipman, D. W., et al. (2009). Climatological mean and decadal change in surface ocean pCO_2, and net sea-air CO_2 flux over the global oceans. *Deep Sea Research., Part II*, 56, 554–577. https://doi:10.1016/j.dsr2.2008.12.009

Tokoro, T., Hosokawa, S., Miyoshi, E., Tada, K., Watanabe, K., Montani, S., et al. (2014). Net uptake of atmospheric CO_2 by coastal submerged aquatic vegetation. *Global Change Biology*, https://doi: 10.1111/gcb.12543

Wang, X., He, Y., Yuan, X., Chen, H., Peng, C., Zhu, Q., et al. (2017). pCO_2 and CO_2 fluxes of the metropolitan river network in relation to the urbanization of Chongqing, China. *Journal of Geophysical Research: Biogeosciences*, 122, 470–486, https://doi: 10.1002/ 2016JGR003494

Wanninkhof, R. (2014). Relationship between wind speed and gas exchange over the ocean revised. *Limnology and Oceanology: Methods*, 12, 351–362. https://doi: 10.4319/lom.2014.12.351

Wanninkhof, R., Pickers, P. A., Omar, A. M., Sutton, A., Murata, A., Olsen, A., et al. (2019). A surface ocean CO_2 reference network, SOCONET and associated marine boundary layer CO_2 measurements. *Frontiers in Marine Science*, 12. https://doi.org/10.3389/fmars.2019.00400

Weiss, R. F. (1974). Carbon dioxide in water and seawater: The solubility of a non-ideal gas. *Marine Chemistry*, 2, 203–215. https://doi.org/10.1016/0304-4203(74)90015-2

Zeebe, R. E., & Wolf-Gladrow, D. (2001). CO_2 in seawater: Equilibrium, Kinetics, Isotopes. In *Elsevier Oceanography Series* (Vol. 65). Amsterdam: Elsevier.